

---

## ANALYSIS OF CONICAL LOG-PERIODIC ANTENNAS

**Thorsten W. Hertel<sup>1</sup> and Glenn S. Smith<sup>2</sup>**

<sup>1</sup> Time Domain Corporation  
Cummings Research Park  
7057 Old Madison Pike  
Huntsville, AL 35806

<sup>2</sup> School of Electrical and Computer Engineering  
Georgia Institute of Technology  
Atlanta, GA 30332-0250

*Received 5 July 2002*

**ABSTRACT:** In this paper, a new log-periodic antenna design is investigated using the finite-difference time-domain method. The two-arm, conical log-periodic antenna is linearly polarized and has uniform performance characteristics over a broad range of frequencies. It is shown that the shape of the antenna arms has a significant impact on the performance and the bandwidth of the antenna. © 2003 Wiley Periodicals, Inc. Microwave Opt Technol Lett 36: 28–32, 2003; Published online in Wiley InterScience (www.interscience.wiley.com). DOI 10.1002/mop.10661

**Key words:** *log-periodic antenna; broadband antenna*

### 1. INTRODUCTION

There are several applications in telecommunications, electromagnetic compatibility, and radar that require broadband antennas—antennas with uniform performance characteristics over a broad range of frequencies. Rumsey showed that practical antennas with broad bandwidth can be designed by following certain geometrical guidelines [1]. Two of the most popular designs based on these guidelines are the planar and conical spiral antennas. The performance aspects of these antennas, such as impedance, gain, and

This work was supported by the John Pippin Chair in Electromagnetics at Georgia Tech.

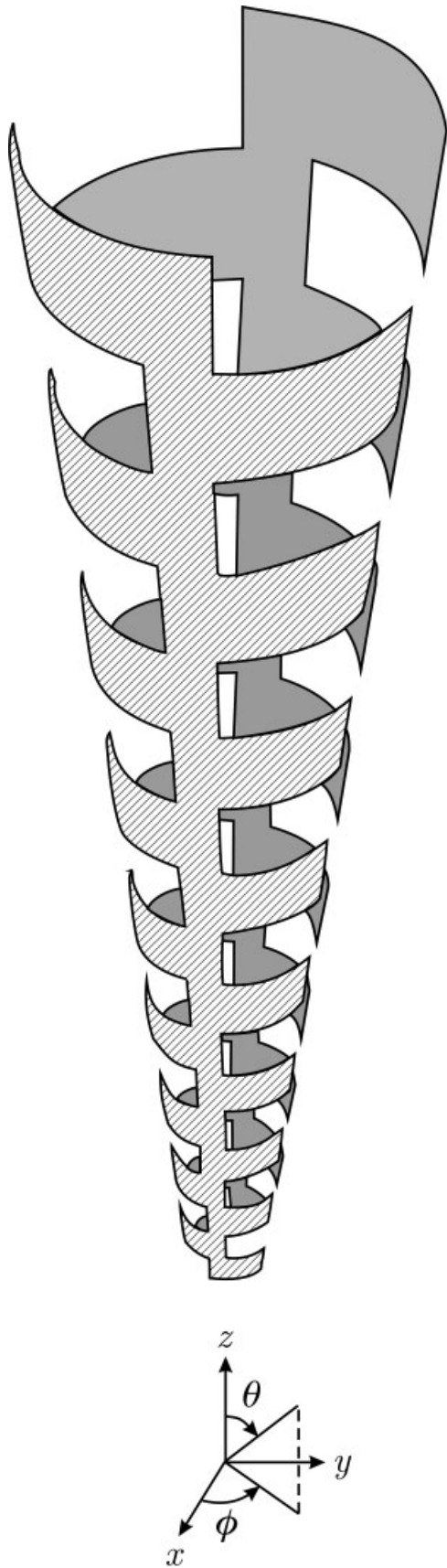


**Figure 1** Schematic drawing for the two-arm, conical log-periodic antenna with rectangular teeth

pattern, have been extensively studied and documented with design graphs based on empirical results [2, 3] and accurate numerical analysis [4].

The objective of this paper is to present a new broadband log-periodic antenna with high directive gain, good match, and linear polarization: the conical log-periodic antenna. This antenna is derived from the conical spiral antenna introduced by Dyson [3] and the planar log-periodic antennas introduced by DuHamel and Isbell [5]. It is shown schematically in Figure 1. Like all frequency-independent antennas, the geometry of this antenna is mainly described by angles, and lengths are introduced to specify the smallest and largest dimensions of the (finite) antenna.

In section 2, the antenna geometry is presented, including various antenna arm designs, and the modeling of the antenna using the finite-difference time-domain (FDTD) method is briefly described. Results for the impedance, gain, and pattern are then presented in section 3.

## 2. ANTENNA GEOMETRY AND FDTD MODELING

The two-arm, conical log-periodic antenna, shown in Figure 1, consists of two metallic strips or arms placed on the surface of a cone. A practical approach for constructing this antenna is shown schematically in Figure 2(a). The metallic arms are formed on a

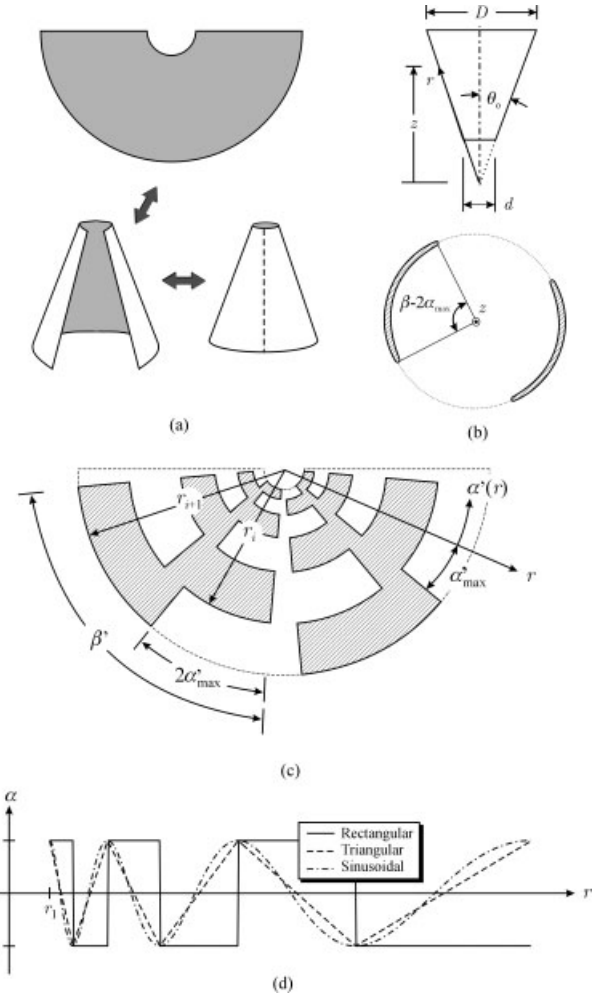


**Figure 2** (a) Schematic drawing showing the fabrication of the antenna; (b) side view and top view of the basic cone; (c) schematic model of the unwrapped log-periodic antenna ( $\theta_o = 30^\circ$ ); (d) modulation functions for various tooth shapes

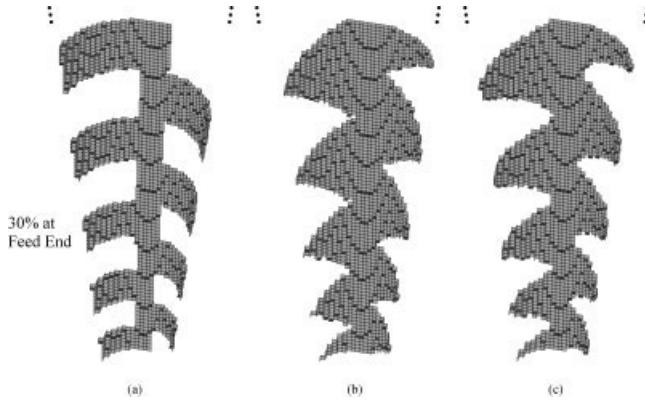


**Figure 3** FDTD model for the conical log-periodic antennas with different tooth modulations: (a) rectangular; (b) triangular; (c) sinusoidal. Only 30% of one arm of the antenna at the feed end is shown

planar, flexible circuit board through a wet chemical etch. The circuit board is then wrapped around a conical mandrel, and soldered or taped along its seam. The basic cone, shown in Figure 2(b), is characterized by the half angle of the cone  $\theta_o$  and the diameters  $d$  and  $D$  that limit the extent of the antenna at the small and large ends. In Figure 2(c), the antenna arm geometry is shown on the planar sector obtained by unwrapping the conical antenna. This drawing is for the angle  $\theta_o = 30^\circ$ . Simple geometry shows that any angular width  $\chi'$  on the planar sheet translates into an angular width  $\chi$  on the conical structure using the relation

$$\chi' = \chi \sin \theta_o. \quad (1)$$

Hence, as shown in Figure 2(c), the total angular width of the unwrapped cone is  $180^\circ$  when  $\theta_o = 30^\circ$ .

For the design shown in Figure 2(c) the notches and teeth of constant angular width  $2\alpha'_{\max}$  are inscribed in the circular sector of angular width  $\beta'$ . Based on the principles of log-periodic antennas, the dimensions of these notches/teeth vary periodically, in particular, the radii measured from the apex to two adjacent edges of an arm are related to each other by

$$\frac{r_{i+1}}{r_i} = \kappa, \quad (2)$$

where  $\kappa$  is the geometric ratio for the log-periodic antenna. On the cone, the second arm is symmetrically located to the first (diametrically opposite), and at any height  $z$  the angular width of an antenna arm is  $\beta - 2\alpha_{\max}$ . All of the designs presented here are for the case  $\beta - 2\alpha_{\max} = 90^\circ$ , which is shown in Figure 2(c) for the unwrapped case\* and in the bottom of Figure 2(b) for a planar cut through the conical antenna. For this choice of angles, the metallic arms are identical in size and shape to the open regions.

The main objective of this work is to study the effect of different tooth shapes on antenna performance. To describe the modulation of the teeth, the angle  $\alpha(r)$  is introduced (see Fig. 2(c)). Since we assume that the minimum and maximum values of the modulation angle  $\alpha(r)$  are independent of the radius  $r$ , this angle is measured from the center of the sector (with angular width  $2\alpha_{\max}$ ) that makes up the tooth geometry, so that  $\alpha(r_i) = \pm\alpha_{\max}$ . The modulation angle  $\alpha(r)$  for the rectangular tooth geometry is

$$\alpha_{\text{rect}}(r) = \alpha_{\max} \sum_{i=1}^N \Pi\left(\frac{r - r_i}{r_{i+1} - r_i}\right)(-1)^{i-1}, \quad (3)$$

for the triangular tooth geometry

$$\alpha_{\text{tri}}(r) = \alpha_{\max} \sum_{i=1}^N \Lambda\left(\frac{r - r_i}{r_{i+1} - r_i}\right)(-1)^{i-1}, \quad (4)$$

and for the sinusoidal tooth geometry

$$\alpha_{\text{sin}}(r) = -\alpha_{\max} \cos[\pi + \pi \log(r/r_1)/\log \kappa]. \quad (5)$$

In Eqs. 3 and 4, we used the following definitions for the one-sided step function and the triangular function:

$$\Pi(\xi) = \begin{cases} 1, & 0 \geq \xi \leq 1 \\ 0, & \text{otherwise} \end{cases} \quad (6)$$

$$\Lambda(\xi) = \begin{cases} 1 - 2\xi, & 0 \geq \xi \leq 1 \\ 0, & \text{otherwise} \end{cases} \quad (7)$$

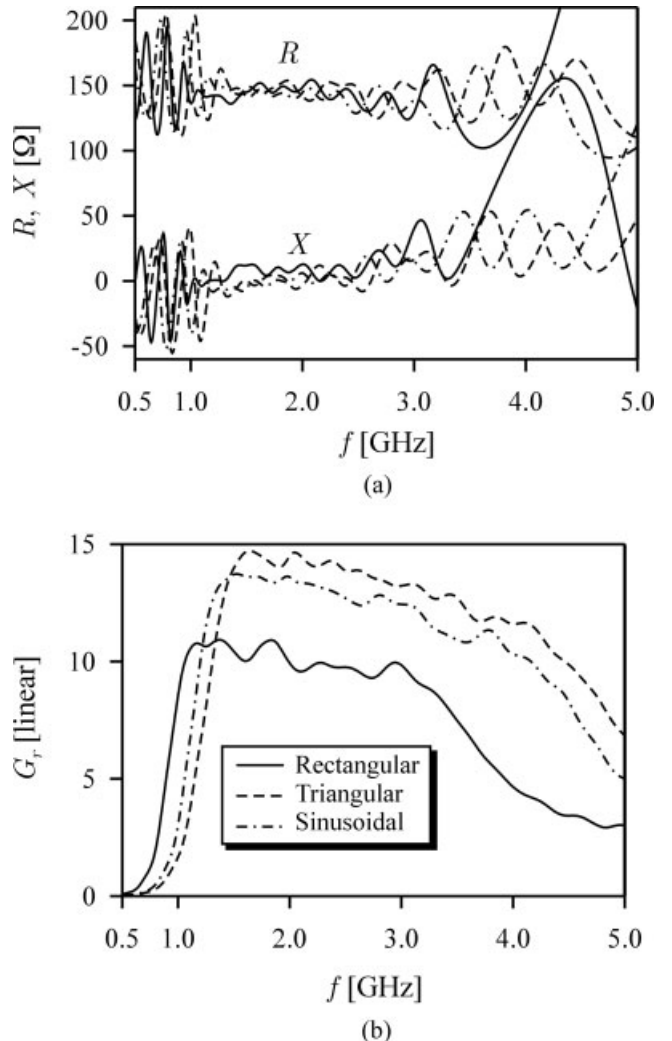


**Figure 4** Results for (a) input impedance and (b) realized gain on the axis for the  $\phi$  component of the electric field

\* As described earlier, the characteristic equation  $\beta - 2\alpha_{\max} = 90^\circ$  transforms into  $\beta' - 2\alpha'_{\max} = 90^\circ \sin \theta_o$  when measured on the unwrapped surface.

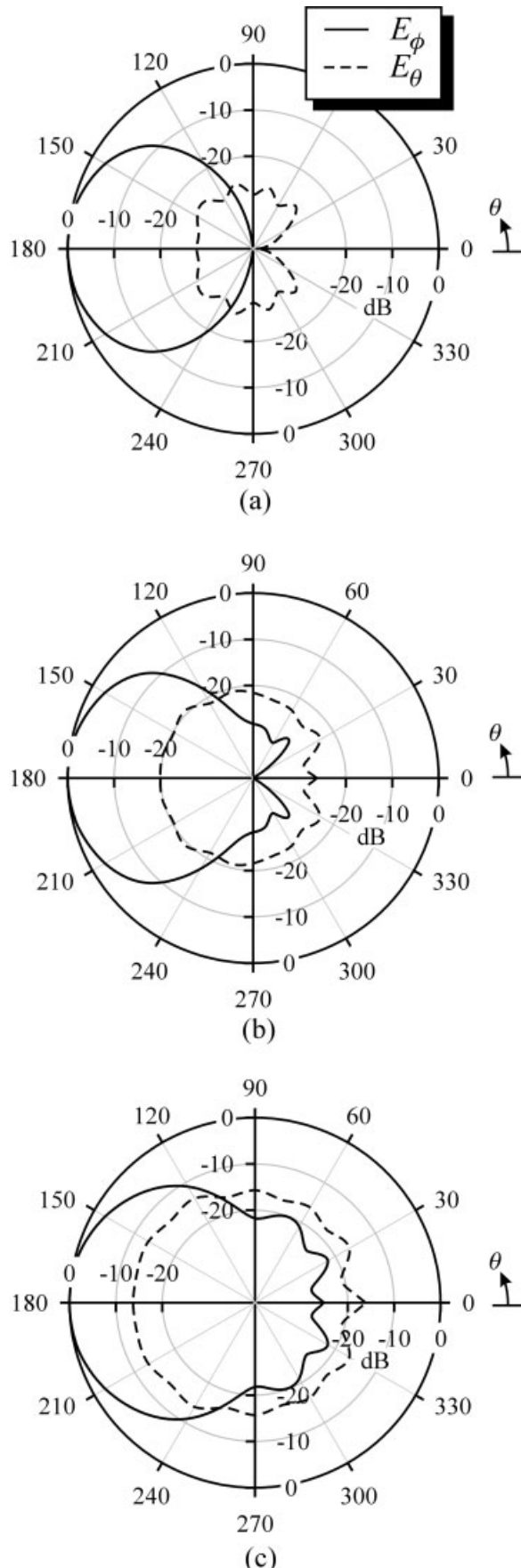


**Figure 5** Far-zone patterns ( $\phi = 0^\circ$ ) for the electric field radiated by the antenna with sinusoidal teeth at the frequencies: (a)  $f = 1.5$  GHz; (b)  $f = 3.0$  GHz; (c)  $f = 4.5$  GHz

with  $r_i = r_1 \kappa^{i-1}$  the  $i$ th peak and  $N$  the total number of peaks. Here,  $r_1 = d/(2 \sin \theta_o)$  is the distance from the apex of the cone to the small end of the antenna (diameter  $d$ ).

The numerical results for the impedance, gain, and pattern are obtained using a full electromagnetic analysis of the antenna performed with the FDTD method. The details for the analysis are similar to those for the analysis of the conical spiral antenna, which were presented earlier [4]. In this analysis, the computational domain is discretized using cubic cells with  $\Delta x = \Delta y = \Delta z = 1.25$  mm, which corresponds to 48 cells per wavelength at the highest frequency investigated ( $f_{\max} = 5$  GHz). Figure 3 shows the staircased surfaces that model the conical log-periodic antennas with (a) rectangular, (b) triangular, and (c) sinusoidal tooth geometry. For clarity, only a small portion (about 30%) of one arm of the antenna near the drive point is shown.

The space surrounding the antenna is truncated with the perfectly-matched-layer (PML) absorbing boundary condition. The antenna is fed at the small end with a transmission-line (the so-called transmission-line feed), and it is terminated at the large end with a resistive disc to reduce reflections. The excitation is the differentiated Gaussian pulse

$$v_{\text{inc}}(t) = -V_0 \left( \frac{t}{\tau_p} \right) e^{0.5-0.5(t/\tau_p)^2}, \quad (8)$$

where  $\tau_p$  is the characteristic time for the pulse. This pulse has the advantage that it does not contain a zero-frequency component, which can cause long settling times in the simulation. The frequency-domain results are obtained by Fourier transforming the time-domain signals.

### 3. RESULTS

The numerical results presented in this section are for conical log-periodic antennas with the three tooth geometries introduced earlier. The antennas have a half angle of the cone of  $\theta_o = 7.5^\circ$ , total angular width of the arms  $\beta = 160^\circ$ , maximum modulation angle  $\alpha_{\max} = 35^\circ$ , geometric ratio  $\kappa = 1.105$ , and ratio of maximum to minimum diameter of the cone  $D/d \pm 6$ , with  $d = 2$  cm. Other designs were investigated, for example, different values of  $\beta$ ,  $\alpha_{\max}$ , and  $\kappa$ ; however, the above geometry gave the best results in terms of impedance match and realized gain (gain including mismatch). The antennas are fed from a transmission line with characteristic impedance  $Z_c = 100 \Omega$ , and they are terminated at the large end with a thin disc of resistive material (resistance per square  $R_s = 150 \Omega$ ) [4].

The input impedance is shown as a function of frequency in Figure 4(a). The antennas with the triangular and sinusoidal tooth shapes are clearly seen to be better matched to the transmission line, namely, these antennas have an almost constant resistance ( $R \approx 150 \Omega$ ) with a small reactance ( $|X| \approx 0$ ) for frequencies  $f \leq 4.7$  GHz, while the antenna with the rectangular teeth has similar characteristics only for frequencies  $f \leq 3.5$  GHz. The realized gain for the  $\phi$  or  $y$  component of the electric field in the main radiation direction ( $\theta = 180^\circ$ ,  $\phi = 0^\circ$ ) is shown in Figure 4(b) on a linear scale. Again, the antennas with the triangular and sinusoidal teeth clearly outperform the antenna with the rectangular teeth for frequencies  $f > 1.1$  GHz. Based on the results in Figure 4, we assume that for the antennas with the sinusoidal and triangular teeth, the upper and lower limits of the operational frequency range are determined by the realized gain. When the bandwidth of the antenna, BW, is defined by the frequencies at which the realized gain drops to one half (-3 dB) of its maximum value, the bandwidth for the antenna with sinusoidal teeth is  $BW \approx 4.7$  GHz/

$1.1 \text{ GHz} \approx 4.3$ , and that for the antenna with triangular teeth is  $\text{BW} \approx 4.9 \text{ GHz}/1.2 \text{ GHz} \approx 4.1$ . Additional calculations show that within the bandwidth of operation the realized gain for the  $\phi$  component of the electric field is greater than that for the  $\theta$  component of the electric field by at least one order of magnitude. Hence, for practical purposes, the antenna is linearly polarized on axis.

Figure 5 shows vertical-plane ( $\phi = 0^\circ$ ), far-zone field patterns for the antenna with the sinusoidal teeth at three frequencies within the operational bandwidth: (a)  $f = 1.5 \text{ GHz}$ , (b)  $f = 3.0 \text{ GHz}$ , and (c)  $f = 4.5 \text{ GHz}$ . Patterns are given for the two orthogonal components of the electric field, namely, the  $\phi$  component (solid line) and the  $\theta$  component (dashed line). For this antenna, the  $\phi$  component of the field in the forward direction ( $-\hat{z}$ , see Fig. 1) is clearly dominant, and the radiation is concentrated near the direction  $\theta = 180^\circ$ . Hence, this antenna predominantly radiates linear polarization unidirectionally towards the apex of the cone.

#### 4. CONCLUSION

The conical, log-periodic antenna was analyzed using the FDTD method. Three different tooth shapes for the antenna were investigated: rectangular, triangular, and sinusoidal. These new antennas were shown to be broadband with uniform input impedance, gain, and pattern. The antennas with the triangular and sinusoidal teeth were seen to clearly outperform the antenna with rectangular teeth.

#### REFERENCES

1. V.H. Rumsey, Frequency independent antennas, Academic Press, New York, 1966.
2. J.D. Dyson, The equiangular spiral antenna, IRE Trans Antennas Propagat AP-7 (1959), 181–187.
3. J.D. Dyson, The characteristics and design of the conical log-spiral antenna, IEEE Trans Antennas Propagat AP-13 (1965), 488–499.
4. T.W. Hertel and G.S. Smith, Analysis and design of two-arm conical spiral antennas, IEEE Trans Electromagn Compat 44 (2002), 25–37.
5. R.H. DuHamel and D.E. Isbell, Broadband logarithmically periodic antenna structures, IRE Natl Convention Rec (1957), 119–128.

© 2003 Wiley Periodicals, Inc.